Molecular Therapy
Oncolytics
Original Article

AMERICAN SOCIETY of GENE & CELL THERAPY

Combination Therapy with Reovirus and ATM Inhibitor Enhances Cell Death and Virus Replication in Canine Melanoma

Masaya Igase,[1] Shusaku Shibutani,[2] Yosuke Kurogouchi,[3] Noriyuki Fujiki,[3] Chung Chew Hwang,[1] Matt Coffey,[4] Shunsuke Noguchi,[5] Yuki Nemoto,[1,3] and Takuya Mizuno[1,3]

[1]Laboratory of Molecular Diagnostics and Therapeutics, The United Graduate School of Veterinary Science, Yamaguchi University, Yamaguchi, Japan; [2]Laboratory of Veterinary Hygiene, Joint Faculty of Veterinary Medicine, Yamaguchi University, Yamaguchi, Japan; [3]Laboratory of Molecular Diagnostics and Therapeutics, Joint Faculty of Veterinary Medicine, Yamaguchi University, Yamaguchi, Japan; [4]Oncolytics Biotech Inc., Calgary, AB, Canada; [5]Laboratory of Veterinary Radiology, Graduate School of Life and Environmental Sciences, Osaka Prefecture University, Osaka, Japan

Oncolytic virotherapy using reovirus is a promising new anti-cancer treatment with potential for use in humans and dogs. Because reovirus monotherapy shows limited efficacy in human and canine cancer patients, the clinical development of a combination therapy is necessary. To identify candidate components of such a combination, we screened a 285-compound drug library for those that enhanced reovirus cytotoxicity in a canine melanoma cell line. Here, we show that exposure to an inhibitor of the ataxia telangiectasia mutated protein (ATM) enhances the oncolytic potential of reovirus in five of six tested canine melanoma cell lines. Specifically, the ATM inhibitor potentiated reovirus replication in cancer cells along with promoting the lysosomal activity, resulting in an increased proportion of caspase-dependent apoptosis and cell cycle arrest at G2/M compared to those observed with reovirus alone. Overall, our study suggests that the combination of reovirus and the ATM inhibitor may be an attractive option in cancer therapy.

INTRODUCTION

Canine melanoma is among the most aggressive cancers, exhibiting the ability to readily metastasize to other organs such as the lung, lymph nodes, and liver. Naturally occurring canine melanoma is considered a pre-clinical model of human melanoma.[1,2] Therefore, new therapeutic approaches with efficacy against canine cancers have potential for application in the treatment of human cancers.

Oncolytic virotherapy has been studied extensively in human cancers. In 2015, a gene-modified herpes simplex virus-1, talimogene laherparepvec (T-VEC), was approved by the U.S. Food and Drug Administration (FDA) as a treatment for melanoma in patients with unresectable lesions of the skin and lymph nodes.[3] Oncolytic viruses are considered attractive treatment options because such reagents are known to activate anti-tumor innate and/or adaptive immune effector cells.[4–7] Indeed, multiple clinical trials have examined the efficacy against human cancers of oncolytic viruses in combination with chemotherapeutic drugs, radiation, and small molecule inhibitors.[8–10] New candidate drugs for use in combination therapy with oncolytic viruses for treating human cancers still need to be identified.

In the veterinary field, there have been only a limited number of reports regarding the use of oncolytic viruses against canine cancer, but several pre-clinical trials suggesting possible application in human medicine have been reported recently.[11–14] Reovirus is a double-stranded RNA virus with low pathogenicity in humans. Our laboratory has previously reported that REOLYSIN, a good manufacturing practice (GMP)-grade non-modified reovirus serotype 3 Dearing strain reovirus, exhibits efficacy in the treatment of canine cancers including mast cell tumors, lymphoma, mammary gland tumors, and melanoma when tested *in vitro* and *in vivo* in mouse xenograft models.[15–18] We also have carried out pilot clinical studies using REOLYSIN to treat 19 dogs with spontaneously occurring tumors, demonstrating that reovirus therapy was safe and well-tolerated in tumor-bearing dogs.[19] Although decreased tumor volume was observed in some of the reovirus-treated dogs, complete tumor regression was not seen in any of the enrolled dogs. REOLYSIN has been used in multiple clinical trials in human cancer patients, primarily in combination with chemotherapeutic agents, with the intent of enhancing the efficacy of oncolytic therapy.[10,20] In general, other therapeutic options are needed to enhance reovirus oncolysis for the treatment of dogs and humans with tumors.

Therefore, the objective of our current study was to develop a new combination approach for oncolytic virotherapy using reovirus in canine cancers. By screening a large number of small molecule inhibitors in combination with reovirus, we successfully identified a novel

Received 13 November 2018; accepted 16 August 2019;
https://doi.org/10.1016/j.omto.2019.08.003.

Correspondence: Takuya Mizuno, DVM, PhD, Laboratory of Molecular Diagnostics and Therapeutics, Joint Faculty of Veterinary Medicine, Yamaguchi University, 1677-1 Yoshida, Yamaguchi 753-8515, Japan.
E-mail: mizutaku@yamaguchi-u.ac.jp

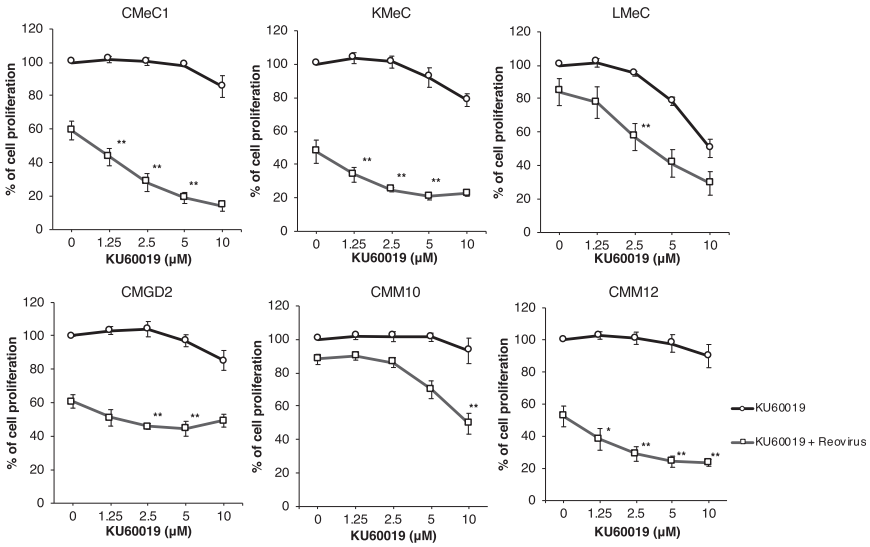

Figure 1. ATM Inhibitor KU60019 Enhances Reovirus-Induced Cell Growth Inhibition in Canine Melanoma Cell Lines

To evaluate cell proliferation, canine melanoma cell lines (CMeC1, KMeC, LMeC, CMM10, CMM12, and CMGD2) were treated with reovirus (MOI 100 for all cell lines except CMGD2 at MOI 10) and KU60019 (indicated concentration) for 48 h before adding CCK-8 reagent. Data are expressed as the mean ± SD from at least three independent experiments. p values were calculated for the comparison between reovirus alone and reovirus combined with KU60019. To focus on the additional effects provided by KU60019, significance was tested only where no significant difference was observed between mock control and KU60019 alone. Tukey-Kramer test, *$p < 0.05$, **$p < 0.01$.

inhibitor of the ataxia telangiectasia mutated protein (ATM). Here, we report the first evidence to our knowledge that the cytotoxicity of reovirus is potentiated by inhibition of ATM in canine melanoma cell lines. We also show that ATM inhibition increases reovirus replication, endosomal acidification, and cathepsin B activity. Notably, reovirus was able to induce the phosphorylation of ATM without inducing DNA damage. Thus, our study demonstrated that the combination of reovirus and an ATM inhibitor may be an attractive option in cancer therapy.

RESULTS

The Combination of an ATM Inhibitor and Reovirus Enhances Anti-tumor Effects in Cell Lines

To identify drugs that enhance reovirus-induced anti-tumor effects, we screened a 285-compound signaling pathway inhibitor library for activity in the CMeC1 canine melanoma cell line (Figure S1). This screen revealed that the ATM inhibitor KU55933 showed no effect on cell proliferation by itself but potentiated the cytotoxicity of reovirus when used in combination with reovirus. Moreover, the combination of KU55933 and reovirus yielded dose-dependent suppression of CMeC1 cell growth (Figure S2). For subsequent experiments, a higher specificity inhibitor of the ATM, KU60019[21] was used in place of KU55933.

To confirm if KU60019 enhances reovirus-induced anti-tumor effects in other types of canine melanoma cell lines, we also examined *in vitro* cell survival using another five canine melanoma cell lines (Figure 1). KU60019 combined with reovirus (MOI 100) significantly suppressed cell proliferation in CMeC1, KMeC, CMM12, LMeC, and CMM10 cell lines, as shown with KU55933. These results indicated that the combination of KU60019 and reovirus yielded significant cell growth inhibition compared to compound or virus alone in five of six tested canine melanoma cell lines excepting CMGD2. These data provided evidence that combination treatment with reovirus and ATM inhibitor potentiated anti-tumor activity in canine melanomas.

To confirm the specificity of the ATM inhibitor, the ATM-encoding gene was knocked out in several canine melanoma cell lines (CMeC1, KMeC, CMM10, and CMM12) using a CRISPR/Cas9-based system (Figure 2A). At 48 h after infection with reovirus, *ATM* knockout cells showed greater inhibition of cell viability than did the respective ATM^+ cells (Figure 2B). Whereas the *ATM* knockout did not influence on the cell growth in CMeC1 and CMM10 compared to ATM^+ (wild-type) cells, but the growth of KMeC and CMM12 were suppressed to some extent (Figure S3). These results supported that inhibition of ATM sensitizes canine melanoma cell lines to reovirus-induced cytotoxicity.

KU60019 Enhances Reovirus-Induced Apoptosis and Cell Cycle Arrest

Next, we assessed the potential mechanism by which the combination of KU60019 and reovirus induces anti-tumor effects. In addition to cell proliferation assay, cell viability was examined in four of these cell lines (CMeC1, KMeC, LMeC, and CMGD2) by means of a trypan blue exclusion test (Figure 3A). Compared to reovirus alone, the combination of KU60019 and reovirus strongly potentiated cell death in three of the four canine melanoma cell lines, excepting CMGD2. At the earlier time point (24 h), cleaved caspase-3 accumulated to higher levels in CMeC1 cells subjected to the combination treatment than in the same cell line treated with reovirus alone (Figure 3B). As expected, the percentage of sub-G1 cells increased from 24 h to 48 h in CMeC1 cells subjected to the combination treatment compared to the percentage in cells treated with reovirus alone (Figure 3C). Notably, pre-treatment of CMeC1 and KMeC with 50 μM Z-VAD-FMK (carbobenzoxy-valyl-alanyl-aspartyl-[O-methyl]-fluoromethylketone, an irreversible caspase inhibitor), before exposure to the combination of reovirus and KU60019, resulted in the complete inhibition of reovirus-induced cell death, as assessed by the trypan blue exclusion test (Figure 3D). However, in a cell proliferation assay, the combination treatment was not sufficient to completely abrogate cell growth in either of these cell lines (Figure 3E). Therefore, we inferred that the

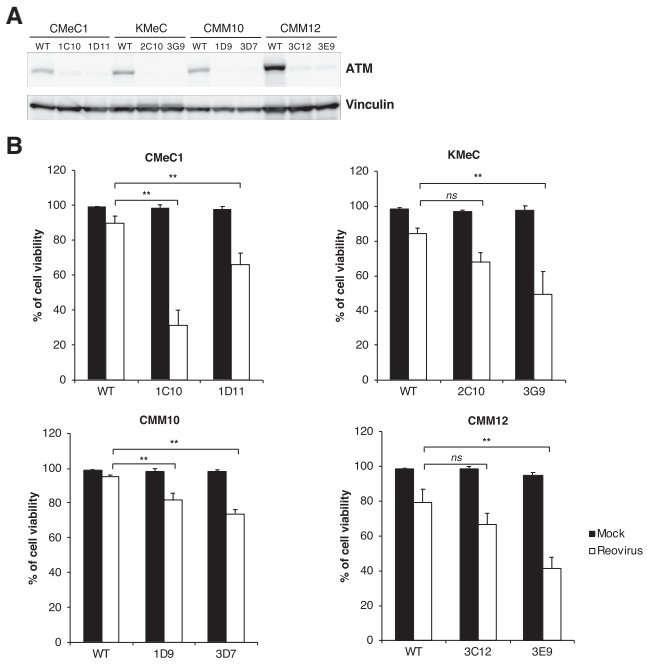

Figure 2. Reovirus Susceptibility Is Enhanced by *ATM* Knockout

(A) The accumulation of ATM in the indicated melanoma cell lines was examined by western blotting. Vinculin was used as a protein loading control. (B) To evaluate cell viability, *ATM* knockout canine melanoma cell lines (CMeC1, KMeC, CMM10, and CMM12) were treated with reovirus (MOI 100) for 48 h before the trypan blue exclusion test. Viable cells and dead cells were counted, and the percentage of viable cells was calculated. Data are expressed as the mean + SD derived from three independent experiments. Tukey-Kramer test, *$p < 0.05$, **$p < 0.01$; ns, not significant.

combination of reovirus and KU60019 also affects cell cycle progression in canine melanoma cells.

Consistent with previous studies showing that reovirus infection results in cell cycle arrest at G2/M in several cancer cell lines,[22–26] we observed that treatment with reovirus alone induced cell cycle arrest at G2/M in CMeC1. Moreover, treatment of CMeC1 with the combination of KU60019 and reovirus resulted in strong cell cycle arrest at G2/M and a reduction of the G1 interval (Figure 4A). In a previous report, the viral nonstructural protein sigma 1 s regulated the activity of CDK1 (the G2/M cyclin-dependent kinase; cdc2), which was required for cell cycle arrest at G2/M.[23] We sought to extend that analysis by using immunoblotting to test treated cells for their levels of CDK1 and p21 (the cyclin-dependent kinase inhibitor) (Figure 4B). After 24 h, cells treated with the combination of KU60019 and reovirus accumulated significantly lower levels of CDK1 than cells treated with either reagent alone. In contrast, the 24-h levels of p21 did not differ significantly among cells treated with the combination or with KU60019 or reovirus alone. Together, these results indicated that the treatment of canine melanoma cells with the combination of KU60019 and reovirus induces both caspase-dependent apoptosis and cell cycle arrest at G2/M.

KU60019 Increases Reovirus Replication and Progeny Virus Number

Next, we assessed the correlation between reovirus replication and anti-tumor effects in canine melanoma cell lines. Western blotting detected reovirus proteins in reovirus-infected CMeC1 and KMeC cells and further revealed that combination treatment (i.e., reovirus infection in the presence of KU60019) yielded increased levels of these proteins at each time point (Figure S4). This analysis was extended by quantifying the progeny virus in the supernatant using the 50% tissue culture infectious dose ($TCID_{50}$) assay. In three of four tested canine melanoma cell lines (CMeC1, KMeC, and CMGD2, but not in LMeC), the combination treatment yielded apparent increases in the number of progeny viruses compared to the input titer (Figure 5A). There was no statistical significance between reovirus alone and combination of KU60019 because the fold increase of virus titer was modest. To prove that viral replication is involved in the cell death effect of the combination of reovirus and KU60019, we used western blotting to assess the accumulation of reovirus structural proteins and cleavage of caspase-3 in CMeC1 subjected to the combination treatment in the presence of ribavirin, an anti-viral reagent.[27] Notably, ribavirin treatment completely suppressed both reovirus replication and caspase-3 cleavage (Figure 5B).

The Combination of KU60019 and Reovirus Does Not Enhance Reovirus Entry

To investigate the biological roles and functions of ATM in the reovirus replication cycle, each step of the replication cycle was analyzed during the treatment with reovirus and ATM inhibitor. The upregulation of junction adhesion molecule (JAM)-A, the reovirus receptor, might be associated with sensitivity to virus-induced cell death.[28,29] The surface expression level of JAM-A was stable on cells treated with KU60019 for 1 h and 24 h by flow cytometric analysis (Figure S5). This data indicated that KU60019 did not influence the step of virus entry.

In addition to testing whether the effect of ATM inhibition was mediated via the proteolytic step of reovirus replication, we examined the enhancement of viral protein expressions using protease-stripped reovirus virions (infectious subviral particles, ISVPs), which are capable of infecting cells lacking virus receptors and cells that have lost their ability to un-coat incoming virions.[30–32] As shown in Figure 5C, combination treatment of reovirus and KU60019 enhanced the expression of reoviral proteins at 12 and 24 h compared to cells exposed to reovirus alone. In contrast, subsequent western blotting (Figure 5D) demonstrated that KU60019 showed no effect on reoviral protein expressions after addition of ISVPs at early time points (at 6 h and 12 h), indicating that KU60019 influences an event before viral disassembly. However, at 24 h, reovirus protein levels were elevated in CMeC1 cells treated with the combination of KU60019 and ISVPs; at 48 h, the combination treatment yielded significant potentiation of cell growth inhibition compared to either component alone (Figure S6), in parallel to the results of Figure 1. We infer that this delayed effect (at 24 h and after) reflects the production of and infection by intact virus after one replication cycle (approximately 18 h[33]),

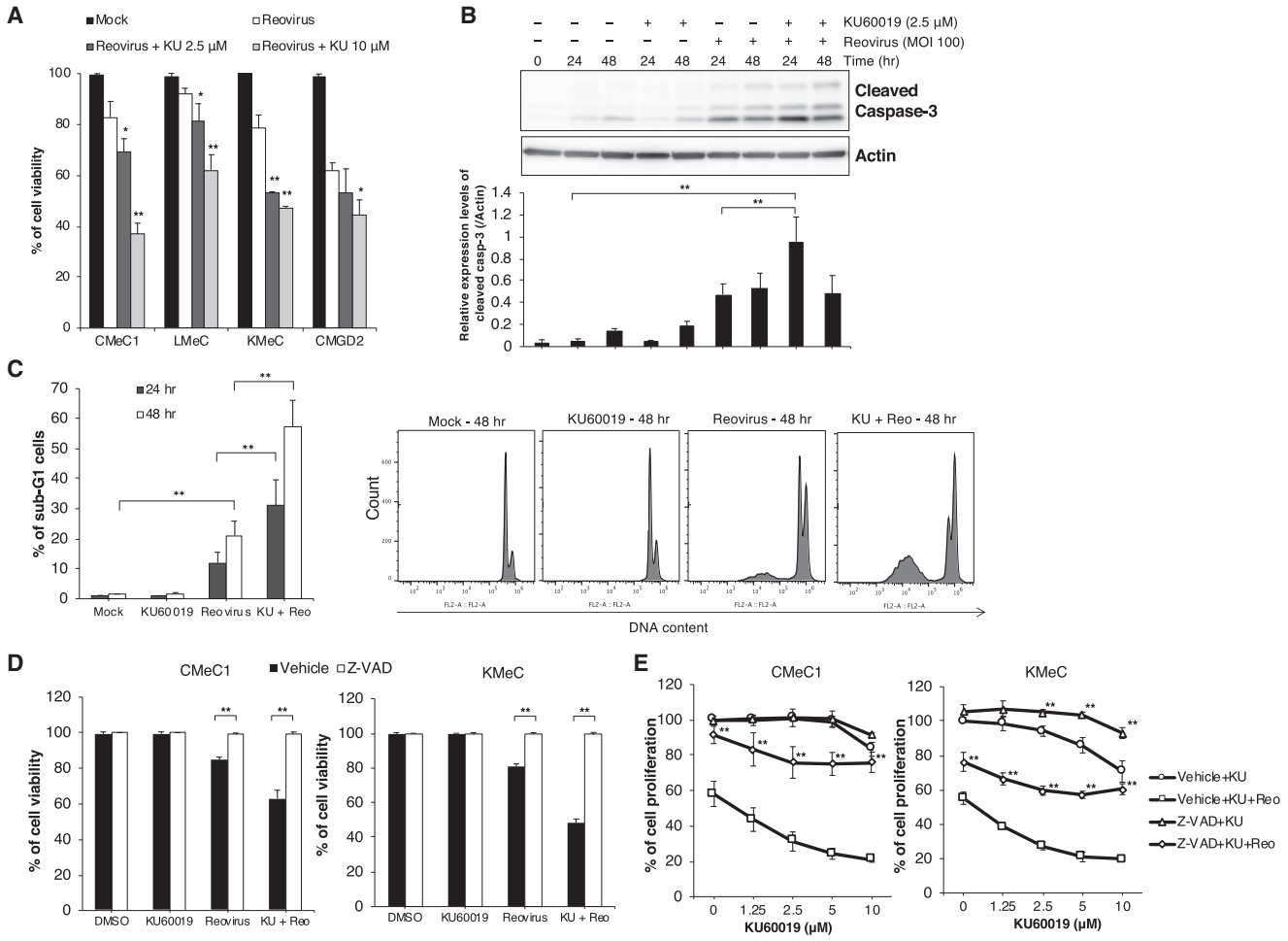

Figure 3. The Combination of KU60019 and Reovirus Induces Apoptotic Cell Death

(A) CMeC1, KMeC, and LMeC were treated with reovirus (MOI 100) and KU60019 (2.5 and 10 μM), and CMGD2 was treated with reovirus (MOI 10) and KU60019 (2.5 and 10 μM). After a 48-h incubation, cell viability was quantified by the trypan blue exclusion test. Data are expressed as the mean ± SD from at least three independent experiments. p values were calculated for the comparison to reovirus alone. Tukey-Kramer test, *$p < 0.05$, **$p < 0.01$. (B) Cleaved caspase-3 levels in CMeC1 treated with reovirus (MOI 100) and KU60019 (2.5 μM) for the indicated time are shown in the upper panel. The relative level of cleaved caspase-3 normalized to actin was quantified from three independent experiments. Data are expressed as the mean + SD. Tukey-Kramer test, *$p < 0.05$, **$p < 0.01$. (C) The sub-G1 population was analyzed in CMeC1 treated with reovirus (MOI 100) and KU60019 (2.5 μM) for 24 and 48 h. The cell numbers and stages were quantified using flow cytometry. The percentage of sub-G1 was calculated in total cells. Data are expressed as the mean + SD derived from three independent experiments. Tukey-Kramer test, *$p < 0.05$, **$p < 0.01$. Histogram of PI staining of each sample at 48 h is shown for representative data from one of three independent experiments. (D and E) The effects of co-treatment for 48 h with Z-VAD-FMK (50 μM) along with the combination of reovirus (MOI 100) and KU60019 (2.5 μM or indicated various concentrations) were quantified using the trypan blue exclusion test (D) or the CCK-8 cell viability assay (E). Data are expressed as the mean ± SD from at least three independent experiments. p values were calculated for the comparison to the vehicle sample. Tukey-Kramer test, **$p < 0.01$.

given that the production of intact virus was potentiated by the combination treatment. These results suggested that outer capsid proteins and the ATM inhibition during the reovirus life cycle might trigger the enhancement of virus replication.

Reovirus Infection Induces the Phosphorylation of ATM without Phosphorylation of DNA Damage-Related Proteins

Infection by some viruses has been shown to induce phosphorylation of ATM, resulting in the induction of DNA damage;[34–36] however, the mechanism linking ATM activity to replication of mammalian reovirus remains unclear. At an early stage of infection (12 h), reovirus induced phosphorylation of ATM in cell line CMeC1, but this modification was abrogated by KU60019 (Figure 6). In addition, we examined whether reovirus induced DNA damage in cancer cells by determining the phosphorylation state of p53, which is known to be regulated by ATM and is known to detect DNA damage.[37] Notably, reovirus did not induce phosphorylation of p53 in a canine melanoma cell line (Figures S7). This observation suggested that

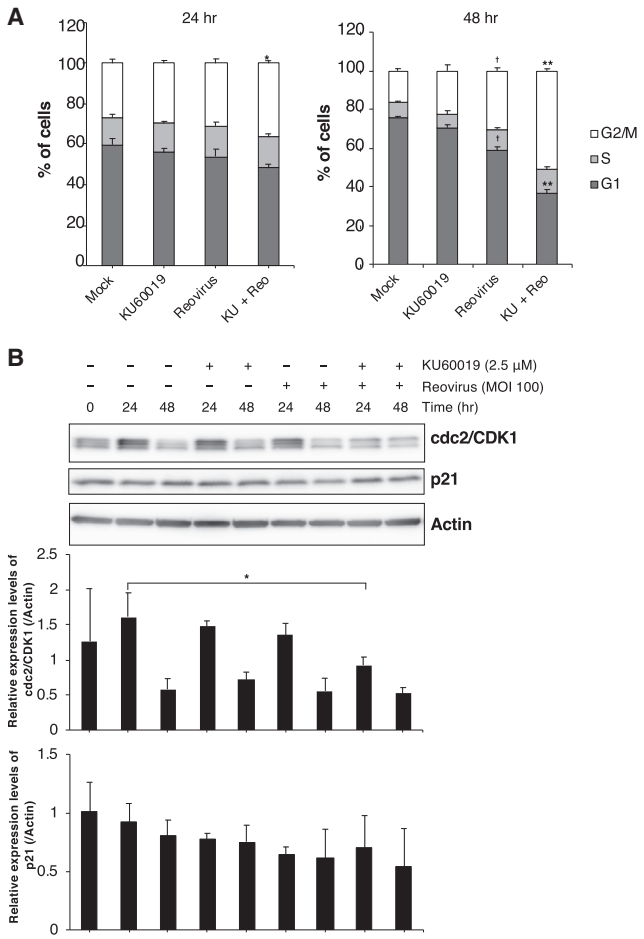

Figure 4. The Combination of KU60019 and Reovirus Induces Cell Cycle Arrest at G2/M and Increases Sub-G1 Populations in Canine Melanoma Cells

(A) CMeC1 was treated with reovirus (MOI 100) and KU60019 (2.5 μM). After 24-h or 48-h incubations, the cell cycle of CMeC1 cells was assessed with propidium iodide (PI) staining, as shown in Figure 3C. Bar graphs indicate the percentages of each cell cycles (G1, S, and G2/M) at 24 h and 48 h in the total cells except sub-G1 populations. p values shown were calculated for the comparison between "Reo" and "KU+Reo." Tukey-Kramer test, *$p < 0.05$, **$p < 0.01$. In addition, p values shown were calculated for the comparison between "mock" and "Reo." Tukey-Kramer test, $^{\dagger}p < 0.01$. (B) cdc2 and p21 protein expression levels in CMeC1 treated as described in (A) are shown in the upper panel. The relative level of each protein normalized to actin was quantified from three independent experiments. Mean + SD are shown. Tukey-Kramer test, *$p < 0.05$, **$p < 0.01$. The membrane in Figure 3B was reprobed and used for this panel.

reovirus infection leads to increases in the phosphorylation of ATM in cancer cells without associated DNA damage, leading to the enhancement of reovirus replication.

Endosomal Acidification and Protease Activity by the Combination of KU60019 and Reovirus

For early phase of infection, disassembly of the reovirus particle in the endosome is required for the replication cycle following internalization of the virus and depends on acidification of the endosome.[38,39] To analyze the effect of the ATM inhibitor on the pH of the endosome, we used LysoTracker red, a dye that exhibits increased fluorescence at the low pH typical of endosomes, lysosomes, or authophagosomes (Figures 7A and 7B). Although the fluorescence intensity of LysoTracker red was not significantly altered compared to mock-treated cells following treatment with either reovirus or KU60019 alone, fluorescence was significantly increased with the combination treatment (Figure 7B). Confocal microscopy confirmed this result, showing that the number of LysoTracker-positive dots was elevated in cells treated with combination of reovirus and KU60019 (Figure 7B). These data suggested that the combination treatment potentiated the acidification of endosomes and lysosomes.

The endosomal acidification modulates the activity of some proteases such as cathepsins.[39–41] Therefore, we evaluated the cathepsin B activity in CMeC1 cells treated as in the above experiments. Unexpectedly, there was little difference in the cathepsin B activity between cells treated with KU60019 for 1 h and combination treatment of reovirus (data not shown). Cells exposed to reovirus alone for 24 h incubation exhibited nominal decreases in cathepsin B activity, although the effect fell short of significance ($p = 0.06$ compared to mock-treated cells; Figure 7C). However, combination treatment restored the level of cathepsin B activity to a value similar to that seen with mock treatment. Even though the effect of the simultaneous treatment with reovirus and KU60019 on cathepsin B activity remains unclear, these results implied that the effect of KU60019 treatment is mediated by enhanced lysosomal activity in the late phase of infection. Thus, combination treatment potentiated the decreased pH in endosomes and lysosomes, followed by activating proteases, but was not committed to enhancing viral proteolysis at the virus entry step during the first round of viral infection.

DISCUSSION

In this study, we screened a drug library to identify new drugs that enhance reovirus cytotoxicity. As a result, we identified an ATM inhibitor. Previous reports demonstrated that many kinds of anticancer drugs have synergistic anti-tumor effects on cancer cells when combined with reovirus.[6,26,42–45] However, the present work represents the first report to our knowledge that an ATM inhibitor can be used as a combination drug with reovirus treatment. Based on our observations, the combinatorial effects of reovirus and the ATM inhibitor resulted in reovirus-related apoptosis and cell cycle arrest at G2/M in most canine melanoma cell lines, with the exception of CMGD2 (a canine melanoma line). The specificity of the ATM inhibitor in our study was supported by a cell survival assay that treated *ATM* knockout canine melanoma cell lines with reovirus. Canine melanoma knockout cell lines exhibited higher susceptibility to reovirus compared to the isogenic wild-type (ATM^{+}) cell lines. However, the cell growth inhibition of reovirus combined with KU60019 was higher than that of reovirus with *ATM* knockout. We hypothesize that KU60019 inhibits not only ATM but also other kinases (members of the phosphatidylinositol 3-kinase [PI3K]-related kinase

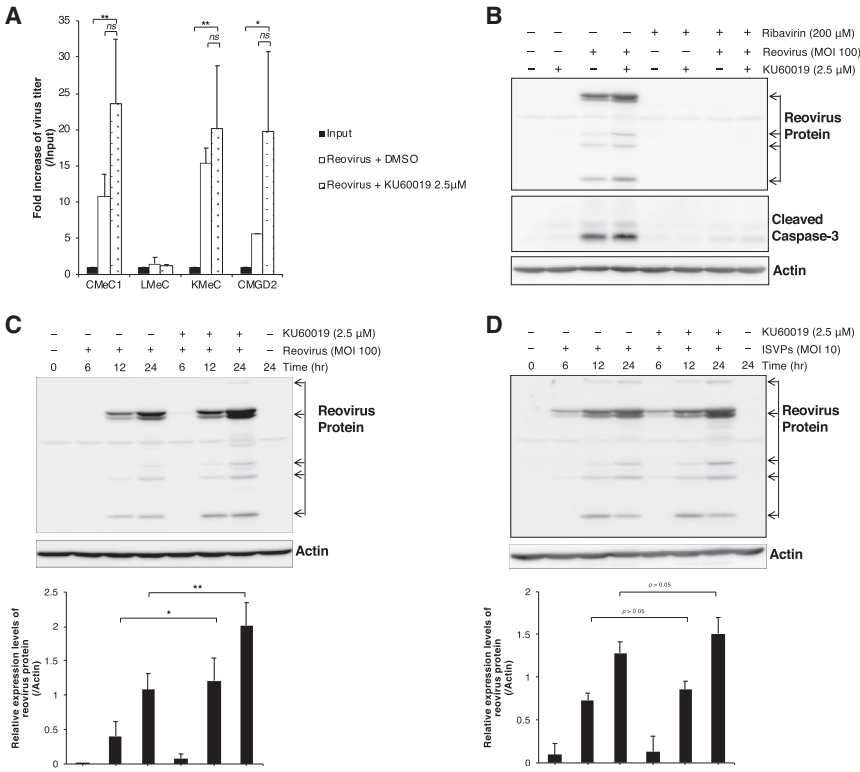

Figure 5. Reovirus Replication Is Enhanced by KU60019 Treatment

(A) Supernatants of reovirus (MOI 100 for CMeC1, KMeC, and LMeC, or MOI 10 for CMGD2)-infected cell lines treated with KU60019 (2.5 μM) were harvested after a 48-hr incubation, and virus titers were determined by the $TCID_{50}$ assay. The fold increase of reovirus titer represents values calculated from the titer of progeny virus divided by the titer of input virus. The mean + SD was calculated from three independent experiments. p values were calculated by Tukey-Kramer test, *p < 0.05, **p < 0.01; ns, not significant. (B) Effects of ribavirin (200 μM) in CMeC1 treated with combination of reovirus (MOI 100) and KU60019 (2.5 μM) for 24 hr were assessed by western blotting using anti-reovirus antibody and anti-cleaved caspase-3 antibody. Actin was used as a protein loading control. (C and D) CMeC1 cells were pre-treated with reovirus virions (C, MOI 100) or ISVPs (D, MOI 10) and washed-out unattached virus followed by treatment with KU60019 (2.5 μM) for the indicated time points. Reovirus structural proteins were detected by western blotting using anti-reovirus polyclonal antibody. Actin was used as a protein loading control. The relative level of reovirus protein normalized to actin was quantified from at least three independent experiments. Mean + SD are shown. Tukey-Kramer test, *p < 0.05, **p < 0.01.

[PIKK] family),[21] in a dose-dependent manner, leading to high-efficiency virus replication and cytotoxicity.

We further examined the effect of the combination treatment on the ATM phosphorylation that is associated with reovirus replication in cancer cells. These experiments were inspired by observations of the effects of human herpes simplex virus-1 (HSV-1), hepatitis C virus, and human immunodeficiency virus-1 infection in other cell lines.[46–49] For those viruses, ATM activation along with DNA damage supports viral replication, such that the inhibition of ATM negatively regulates replication. In contrast, it was unknown whether ATM activation is associated with mammalian reovirus replication. We are aware of only one relevant report, which demonstrated that two ATM-deficient cell lines (L3 lymphoblastoid cells and Granta mantle cell lymphoma cells) were more susceptible to reovirus than were other cell lines.[50] However, the relationship between reovirus replication, oncolysis, and ATM deficiency was not proven in that study. Therefore, in the present work, we identified a putative mechanism for the potentiation of reoviral oncolysis by the normal status and knockout of *ATM*. Interestingly, p53 phosphorylation, a marker of DNA damage, was not observed in canine melanoma cells even though reovirus infection might trigger unknown nuclear damage followed by activation of ATM. To confirm the biological roles and functions of ATM in the reovirus replication cycle, each step of the replication cycle was analyzed. We found that inhibition of ATM enhanced the endosomal acidification and re-activation of protease only in the late phase of reovirus infection. Previous work has shown that endosomal acidification and protease activity are essential for reovirus replication in early time points;[31,39,51] therefore, there might be another mechanism. Reoviridae family members, including mammalian reovirus, facilitate the induction of autophagy, and its autophagy elevates the virus replication.[52–55] To assess the effect of combination treatment of KU60019 and reovirus on autophagy, we have examined the expression levels of the autophagy marker LC3B-II (the lipidated form of LC3B) in CMeC1 and KMeC by western blotting (data not shown). As a result, the accumulation of LC3B-II was observed in canine melanoma cells treated with reovirus alone at 24 h and 48 h, and then treatment of reovirus with KU60019 increased the LC3B-II expression. Although the overall mechanism of virus replication induced by ATM inhibition remains unclear, these data suggested that, at the late phase of infection, combination of reovirus and KU60019 facilitates the induction of autophagy (i.e., the upregulation of cathepsin B activity, the acidification of endosomes and lysosomes, and the LC3B-II accumulation), which might be associated with enhancement of virus replication.

Compared to KU55933 (the library-identified compound), KU60019 has greater specificity and is considered a much improved ATM kinase inhibitor. However, neither KU55933 or KU60019 are suitable for *in vivo* studies, given the low aqueous solubility and low bioavailability of these compounds.[56–58] The ATM inhibitor AZD0156 was recently reported[57] and shown to exhibit superior pharmacokinetics with the potential for oral dosing; this compound is the subject of an ongoing phase I clinical trial being performed by AstraZeneca.

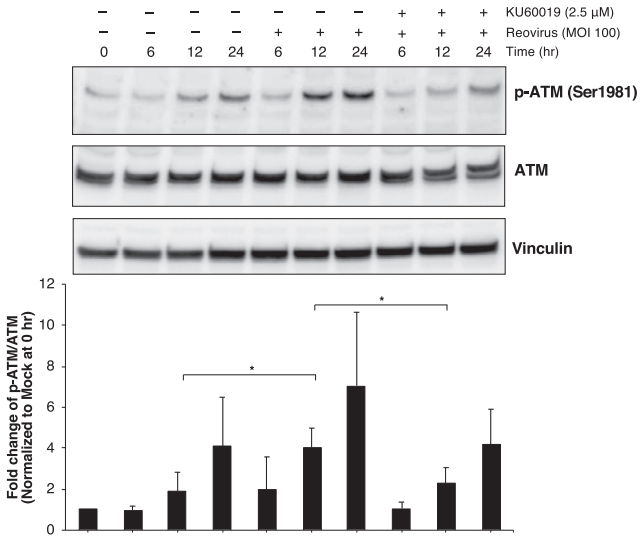

Figure 6. Reovirus Infection Induces the Phosphorylation of ATM in Cancer Cells

Phospho-ATM and total ATM expression levels were assessed by western blotting of lysates from CMeC1 cells treated with reovirus (MOI 100) and KU60019 (2.5 μM) for the indicated times. Vinculin was used as a protein loading control. The graph shows the relative level of each protein (normalized to vinculin) quantified from four independent experiments. The fold change of phospho-ATM divided by total ATM was normalized to the value of mock at 0 h. Mean + SD are shown. Tukey-Kramer test, *$p < 0.05$.

We hope to evaluate the combination of reovirus and AZD0156 in xenograft mice harboring canine melanoma cell lines.

Taken together, our results suggested that the ATM inhibitor KU60019 enhances reovirus-induced anti-tumor effects in canine cancers (Figure 8). This synergy may provide a route to resolving the limited efficacy of reovirus treatment of cancers. Although the mechanism linking ATM activity, endosomal acidification, and reovirus replication remains unknown, we confirmed that treatment with the ATM inhibitor upregulated viral replication, resulting in increased the cell death. Given that the incidence of adverse events may be increased in combination treatment, *in vivo* experiments (e.g., mouse xenograft studies) will be needed to test this combination therapy. Nonetheless, these findings support further investigation of this combination therapy for the treatment of canine cancer patients.

MATERIALS AND METHODS

Cell, Reovirus, and Inhibitors

Seven canine malignant melanoma cell lines (CMeC1, KMeC, LMeC,[59] CMGD2,[60] CMM10, and CMM12[61]) were used in this study. Five of the canine cell lines (CMeC1, KMeC, LMeC, CMM10, and CMM12) were kindly provided by Dr. T. Nakagawa (University of Tokyo, Tokyo, Japan). CMGD2 was kindly provided by Dr. J. Modiano (University of Minnesota, Minneapolis, MN, USA). A mouse L929 fibroblastic cell line (used for the titration of viral progeny) was obtained from the Cell Resource Center for Biomedical Research (Institute of Development, Aging and Cancer, Tohoku University, Sendai, Japan). All cell lines were grown in R10 complete medium (RPMI1640 supplemented with 10% fetal bovine serum [FBS], 100 U/mL penicillin, 100 μg/mL streptomycin, and 55 μM 2-mercaptoethanol) and maintained at 37°C in a humidified 5% CO_2 incubator.

The Dearing strain of reovirus serotype 3 (Reolysin; GMP-grade reovirus) was obtained from Oncolytics Biotech (Calgary, Canada). ISVPs were produced just before use and were generated according to the protocol of Alain et al.[30] In brief, reovirus (2.835×10^8 plaque-forming units [PFU]) was digested with chymotrypsin-HCl (2 μg; Roche Diagnostics, Tokyo, Japan) for 30 min at 37°C. The digestion was terminated by adding phenymethylsulphonyl fluoride (5 mM in ethanol) and shifting the reaction to 4°C.

The ATM inhibitors KU55933 and KU60019 were obtained from AdooQ Bioscience (Irvine, CA, USA).

Drug Screening

To identify the new combination drug, we screened the SCADS inhibitor kit (Ministry of Education, Culture, Sports, Science and Technology, Tokyo, Japan), which includes 285 signaling pathway inhibitors. The canine melanoma cell line CMeC1 (5,000 cells/well) was plated in 96-well plates containing each inhibitor, with or without reovirus at an MOI of 100 PFU per cell, and the plates were incubated for 48 h. After treatment, cell growth inhibition was evaluated by use of the cell counting kit-8 (CCK-8; Dojindo, Kumamoto, Japan) according to the manufacturer's instructions.

Cell Survival Assay

Each cell line was seeded at the density of 5,000 cells (CMeC1, KMeC, LMeC, CMGD2, and CMM12) or 10,000 cells (CMM10) in triplicates in 96-well plates and mock-infected or infected with reovirus at an MOI of 10 or 100 PFU per cell in the presence of the ATM inhibitor KU60019 at 1.25, 2.5, 5.0, or 10 μM; assays were performed in triplicate wells. Cells were cultured for 48 h before adding the CCK-8 reagent. The cell proliferation rate was calculated by measuring absorbance. In the cytotoxicity assay, each cell line was treated with reovirus at an MOI of 100 PFU per cell and KU60019 at 2.5 or 10 μM; assays were performed in triplicate wells. Cells were cultured for 48 h before performing the trypan blue exclusion test.

To assess the inhibition of apoptosis induced by treatment with reovirus and inhibitor, canine melanoma cell lines (CMeC1 and KMeC) were seeded at 5,000 cells per well in 96-well plates. The irreversible pan-caspase inhibitor, Z-VAD-FMK (Calbiochem, Billerica, MA, USA) was added to triplicate wells at a concentration of 50 μM for 1 h before the cells were treated with reovirus (MOI 100) and KU60019 (indicated concentration). After 48 h, cell proliferation and cell viability were evaluated by CCK-8 and trypan blue exclusion test, respectively.

All experiments were repeated at least three times.

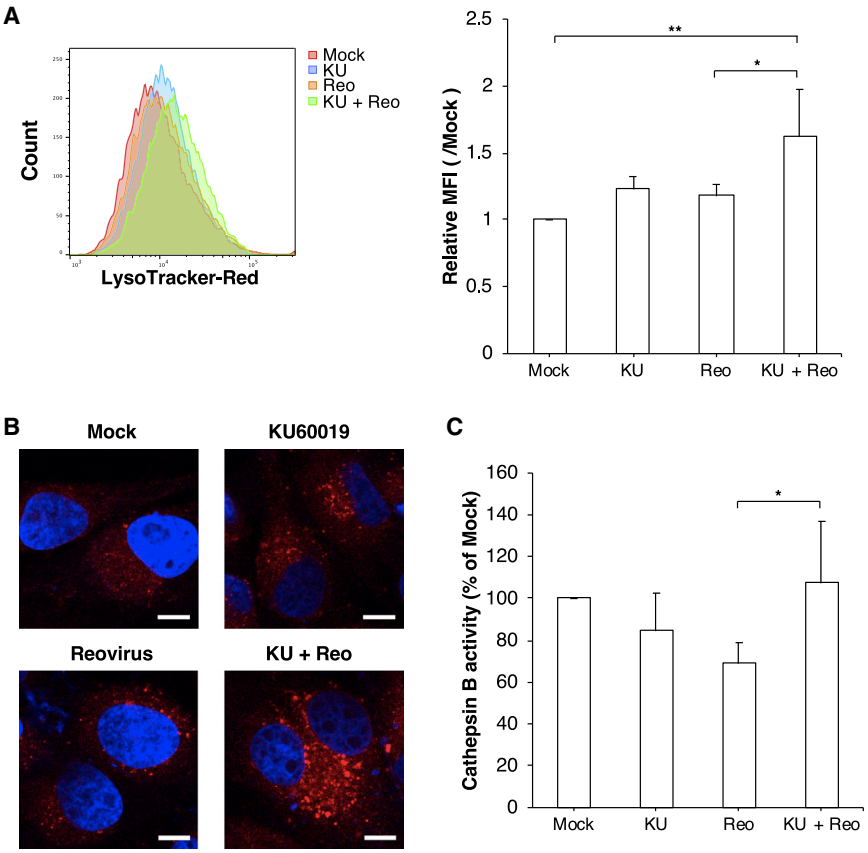

Figure 7. The Combination of Reovirus and KU60019 Promotes the Endosomal Acidification and Activation of Cathepsin B

(A and B) The acidification of endosomes and lysosomes was determined by LysoTracker red staining. CMeC1 cells were treated with reovirus (MOI 100) and KU60019 (2.5 μM) for 24 h before staining. (A) Histogram overlay of LysoTracker red staining of each sample is shown for representative data from one of four independent experiments. Relative median fluorescence intensity (MFI) values relative to mock treatment are indicated. Mean + SD are shown from four independent experiments. Tukey-Kramer test, *$p < 0.05$, **$p < 0.01$. (B) Representative images of samples from each treatment groups are visualized using confocal microscopy at a 100× magnification. Nuclei were stained with DAPI. Scale bars, 10 μm. (C) The enzyme activity of cathepsin B in CMeC1 cells treated as described above was measured and normalized to the value obtained with mock treatment. Mean + SD are shown from five independent experiments. Tukey-Kramer test, *$p < 0.05$.

Reovirus Replication and Progeny Virus

Reovirus replication was examined by western blotting analysis using anti-reovirus antibody (produced by our laboratory[15–18]). Cell lines were seeded at 3×10^5 cells per well in 6-well plates and treated with reovirus (MOI 100) and KU60019 (2.5 μM) for 24 and 48 h. In some experiments examining the reovirus proteins at early stages, wells were rinsed to remove unbound reovirus following adsorption. In brief, CMeC1 was plated at 5×10^5 cells per well in 6-well plates and cultured before use. On the following day, cells were exposed to reovirus (MOI 100) or ISVPs (MOI 10) for 1 h at 4°C. Then, cells were washed and cultured in the presence of KU60019 (2.5 μM) for 6, 12, or 24 h at 37°C. Cells were harvested at the indicated time points and stored at −80°C pending use for western blotting.

Supernatants of the samples from the cytotoxicity assay were collected and stored at −80°C pending use. Viral progeny in the supernatants were measured using the 50% tissue culture dose ($TCID_{50}$) assay on L929 cells, as previously described.[15–18] Titration of the viral progeny was performed on all the supernatants obtained from three independent cytotoxicity assays.

Genome Editing

A small guide RNA (sgRNA) targeting canine *ATM*, 5′-TAGTTT CAGGATCCCGAATC-3′, was designed through the online CRISPR design tool (http://zlab.bio/guide-design-resources); the resulting sgRNA was synthesized and subcloned into the lentiCRISPRv2 plasmid, which was a gift from Dr. Feng Zhang[62] (obtained from Addgene [Cambridge, MA, USA] as accession #52961). The plasmid and packaging vectors were transfected to HEK293T to produce the lentivirus expressing an sgRNA targeting *ATM*. After transduction with the lentivirus, canine melanoma cell lines were cultured in the presence of puromycin (Sigma Aldrich Japan, Tokyo, Japan; 0.6–5.0 μg/ml) to select for stably transduced cells. Individual clones were isolated by the limiting dilution method and further analyzed by western blotting to confirm that the cells no longer produced ATM protein. The resulting clones were used for further experiments.

Flow Cytometric Analysis

To assess the cell cycle distribution, canine melanoma cells (3×10^5 cells/well in 6-well plates) were treated with reovirus (MOI 100) and KU60019 (2.5 μM) for 24 and 48 h. Cells were trypsinized and washed in PBS and fixed in 70% ice-cold ethanol at −30°C for at least 24 h. The fixed cells were re-suspended in PBS supplemented with 0.1 mg/mL of RNase (Nacalai Tesque, Kyoto, Japan) and incubated for 30 min at room temperature. The digested cells then were incubated with 0.1 mg/mL of propidium iodide (PI; Nacalai Tesque) for 5 min and analyzed.

To evaluate surface expression of reovirus receptor JAM-A, a canine melanoma cell line (CMeC1) was seeded at 2×10^5 cells per well in 12-well plates and treated with mock and KU60019 (2.5 μM) for 1 h or 24 h. Incubated cells were stained with primary antibodies including mouse immunoglobulin G1 (IgG1) isotype control (eBioscience) and mouse anti-human JAM-A monoclonal antibody

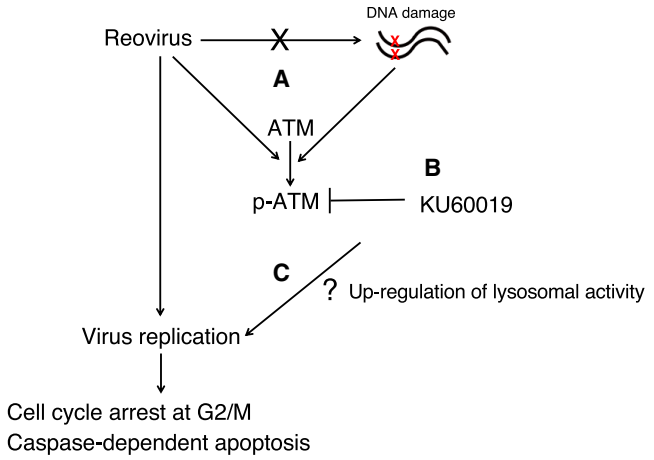

Figure 8. Model of Anti-tumor Effects of Reovirus Combined with KU60019
In general, the phosphorylation of ATM protein is induced when DNA double-strand breaks are caused by UV or radiation. We newly found that reovirus infection activated the ATM protein unaccompanied with DNA double-strand breaks, at the late time points of reovirus infection (after 12 h) (A) (Figure 6). This indicates that reovirus may cause an atypical ATM signaling pathway, which is abrogated by KU60019 (B). The combination treatment of reovirus and KU60019 leads to enhancement the virus replication (C), followed by cell cycle arrest at G2/M and caspase-dependent apoptosis, potentiating anti-tumor effects. However, the mechanism between up-regulation of lysosomal activities and reovirus cytotoxicity is still unknown.

(Santa Cruz), followed by incubation with Dylight488-conjugated goat anti-mouse IgG antibody (BioLegend). Those cells were stained with PI to gate out dead cells.

All stained samples were analyzed using a BD Accuri C6 flow cytometer (BD Biosciences). All given data were analyzed using FlowJo software ver. 10.1 (FlowJo, Ashland, OR, USA).

Western Blotting

Cells were plated at 3×10^5 cells per well in 6-well plates and treated with reovirus (MOI 100) and KU60019 (2.5 μM) for 24 and 48 h. For short-term incubation, CMeC1 cells were plated at 5×10^5 cells per well in 6-well plates, and on the following day, cells were treated as shown above (see Reovirus Replication and Progeny Virus). Harvested cells were lysed at 4°C with NP40 lysis buffer (1% NP40, 10 mM Tris-HCl [pH 7.5], 150 mM NaCl, 1 mM EDTA) supplemented with protease inhibitor cocktails (Nacalai Tesque), 1 mM Na_3VO_4, and 50 mM sodium fluoride (NaF). The resulting supernatants were collected and used as cell lysates. These lysates were subjected to SDS-PAGE, and proteins then were transferred to Hybond polyvinylidene fluoride (PVDF) membrane (GE Healthcare Bio-Sciences, Pittsburgh, PA, USA). The membrane was blocked with Tris-buffered saline (TBS) containing with 0.05% Tween 20 (polyoxyethylene sorbitane monolaureate) and 5% skim milk, followed by addition of the primary antibodies. The primary antibodies are listed in Table S1. Horseradish peroxidase (HRP)-conjugated antibodies were used as the secondary antibodies. The labeled proteins were detected using an enhanced chemiluminescence (ECL) reagent (PerkinElmer). The intensity of the bands was determined by ImageJ software ver. 1.48.

LysoTracker Red Staining

CMeC1 cells (1×10^5 cells) were cultured on microcover glasses (Matunami Garasu Kogyo, Osaka, Japan) in the wells of a 12-well plate. On the following day, cells were exposed to reovirus (MOI 100) for 1 h at 4°C. Then, cells were washed and cultured in the presence of KU60019 (2.5 μM) for 24 h at 37°C. After treatment, cells were incubated with LysoTracker red DND-99 (Invitrogen, Carlsbad, CA, USA) for 30 min at 37°C, followed by fixation with 4% paraformaldehyde. The coverslips were mounted onto glass slides with Molecular Probes prolong gold with DAPI (Invitrogen) for staining of nuclei. Samples were visualized at a 100× magnification using LSM710 confocal microscope (Carl Zeiss, Oberkochen, Germany). Images were analyzed by using ZEN software 2012 (Carl Zeiss). The percentage of LysoTracker red-positive CMeC1 cells was quantified by flow cytometric analysis as described above.

Measurement of Cathepsin B Activity

Cathepsin activity was determined with a cathepsin B activity assay kit (PromoCell, Heidelberg, Germany), according to the manufacturer's instructions. CMeC1 cells were cultured at the density of 5×10^5 cells per well in 6-well plates. Then, cells were treated with reovirus (MOI 100) and KU60019 (2.5 μM) for 24 h. After treatments, cells were lysed with CB cell lysis buffer, followed by mixing with the CB reaction buffer. The cell lysate was incubated at 37°C for 1 h with 200 μM CB substrate Ac-RR-AFC. Cathepsin activity was measured in an ARVO X4 fluorometer (PerkinElmer). The fluorescence values were normalized to values obtained for a mock-treated sample after subtraction of background autofluorescence.

Statistical Analysis

The mean values and SD in each assay were calculated from the mean of at least three biological independent experiments. The significance of differences between samples was determined by the one-way factorial ANOVA test followed by multiple comparison using Tukey-Kramer test. Differences were considered statistically significant if the p values were less than 0.05. Multiple comparison tests were performed using JMP software ver. 9.0 (SAS Institute Japan, Tokyo, Japan).

SUPPLEMENTAL INFORMATION

Supplemental Information can be found online at https://doi.org/10.1016/j.omto.2019.08.003.

AUTHOR CONTRIBUTIONS

M.I. and T.M. conceived the study design and performed all experiments, in addition to writing the paper. S.S. and M.C. provided essential resources and developed methods. Y.K. and N.F. obtained additional data for this study. C.C.H., S.N., and Y.N. analyzed the data and provided critical interpretation. All authors read and approved the final manuscript.

CONFLICTS OF INTEREST

M.C. is president/chief executive officer and has financial interests with Oncolytics Biotech, Inc. The other authors declare no competing interests.

ACKNOWLEDGMENTS

This study was supported by JSPS KAKENHI, grant numbers 15H04598 and 16J06655. We thank the Screening Committee of Anticancer Drugs was supported by a Grant-in-Aid for Scientific Research on Innovative Areas, Scientific Support Programs for Cancer Research, from The Ministry of Education, Culture, Sports, Science and Technology, Japan for providing the SCAD inhibitor kit. Dr. Takayuki Nakagawa (University of Tokyo) and Dr. Jaime Modiano (University of Michigan) kindly provided canine melanoma cell lines to the authors. The authors would like to acknowledge the technical expertise of the DNA Core facility of the Center for Gene Research, Yamaguchi University, supported by a grant-in-aid from the Ministry of Education, Science, Sports and Culture of Japan.

REFERENCES

1. Gillard, M., Cadieu, E., De Brito, C., Abadie, J., Vergier, B., Devauchelle, P., Degorce, F., Dréano, S., Primot, A., Dorso, L., et al. (2014). Naturally occurring melanomas in dogs as models for non-UV pathways of human melanomas. Pigment Cell Melanoma Res. *27*, 90–102.
2. Hernandez, B., Adissu, H.A., Wei, B.R., Michael, H.T., Merlino, G., and Simpson, R.M. (2018). Naturally Occurring Canine Melanoma as a Predictive Comparative Oncology Model for Human Mucosal and Other Triple Wild-Type Melanomas. Int. J. Mol. Sci. *19*, 394.
3. Pol, J., Kroemer, G., and Galluzzi, L. (2015). First oncolytic virus approved for melanoma immunotherapy. Oncoimmunology *5*, e1115641.
4. Marelli, G., Howells, A., Lemoine, N.R., and Wang, Y. (2018). Oncolytic Viral Therapy and the Immune System: A Double-Edged Sword Against Cancer. Front. Immunol. *9*, 866.
5. Filley, A.C., and Dey, M. (2017). Immune System, Friend or Foe of Oncolytic Virotherapy? Front. Oncol. *7*, 106.
6. Rajani, K., Parrish, C., Kottke, T., Thompson, J., Zaidi, S., Ilett, L., Shim, K.G., Diaz, R.M., Pandha, H., Harrington, K., et al. (2016). Combination Therapy With Reovirus and Anti-PD-1 Blockade Controls Tumor Growth Through Innate and Adaptive Immune Responses. Mol. Ther. *24*, 166–174.
7. Mostafa, A.A., Meyers, D.E., Thirukkumaran, C.M., Liu, P.J., Gratton, K., Spurrell, J., Shi, Q., Thakur, S., and Morris, D.G. (2018). Oncolytic Reovirus and Immune Checkpoint Inhibition as a Novel Immunotherapeutic Strategy for Breast Cancer. Cancers (Basel) *10*, 205.
8. Pol, J., Buqué, A., Aranda, F., Bloy, N., Cremer, I., Eggermont, A., Erbs, P., Fucikova, J., Galon, J., Limacher, J.-M., et al. (2016). Trial Watch-Oncolytic viruses and cancer therapy. Oncoimmunology *5*, e1117740.
9. Pol, J., Bloy, N., Obrist, F., Eggermont, A., Galon, J., Cremer, I., Erbs, P., Limacher, J.M., Preville, X., Zitvogel, L., et al. (2014). Trial Watch:: Oncolytic viruses for cancer therapy. Oncoimmunology *3*, e28694.
10. Vacchelli, E., Eggermont, A., Sautès-Fridman, C., Galon, J., Zitvogel, L., Kroemer, G., and Galluzzi, L. (2013). Trial watch: Oncolytic viruses for cancer therapy. Oncoimmunology *2*, e24612.
11. MacNeill, A.L., Weishaar, K.M., Séguin, B., and Powers, B.E. (2018). Safety of an Oncolytic Myxoma Virus in Dogs with Soft Tissue Sarcoma. Viruses *10*, 398.
12. Naik, S., Galyon, G.D., Jenks, N.J., Steele, M.B., Miller, A.C., Allstadt, S.D., Suksanpaisan, L., Peng, K.W., Federspiel, M.J., Russell, S.J., and LeBlanc, A.K. (2018). Comparative oncology evaluation of intravenous recombinant oncolytic Vesicular Stomatitis Virus therapy in spontaneous canine cancer. Mol. Cancer Ther. *17*, 316–326.
13. Gentschev, I., Patil, S.S., Petrov, I., Cappello, J., Adelfinger, M., and Szalay, A.A. (2014). Oncolytic virotherapy of canine and feline cancer. Viruses *6*, 2122–2137.
14. Cejalvo, T., Perisé-Barrios, A.J., Del Portillo, I., Laborda, E., Rodriguez-Milla, M.A., Cubillo, I., Vázquez, F., Sardón, D., Ramirez, M., Alemany, R., et al. (2018). Remission of Spontaneous Canine Tumors after Systemic Cellular Viroimmunotherapy. Cancer Res. *78*, 4891–4901.
15. Hwang, C.C., Umeki, S., Igase, M., Coffey, M., Noguchi, S., Okuda, M., and Mizuno, T. (2016). The effects of oncolytic reovirus in canine lymphoma cell lines. Vet. Comp. Oncol. *14* (*Suppl 1*), 61–73.
16. Igase, M., Hwang, C.C., Coffey, M., Okuda, M., Noguchi, S., and Mizuno, T. (2015). The oncolytic effects of reovirus in canine solid tumor cell lines. J. Vet. Med. Sci. *77*, 541–548.
17. Igase, M., Hwang, C.C., Kambayashi, S., Kubo, M., Coffey, M., Miyama, T.S., Baba, K., Okuda, M., Noguchi, S., and Mizuno, T. (2016). Oncolytic reovirus synergizes with chemotherapeutic agents to promote cell death in canine mammary gland tumor. Can. J. Vet. Res. *80*, 21–31.
18. Hwang, C.C., Umeki, S., Kubo, M., Hayashi, T., Shimoda, H., Mochizuki, M., Maeda, K., Baba, K., Hiraoka, H., Coffey, M., et al. (2013). Oncolytic reovirus in canine mast cell tumor. PLoS ONE *8*, e73555.
19. Hwang, C.C., Igase, M., Sakurai, M., Haraguchi, T., Tani, K., Itamoto, K., Shimokawa, T., Nakaichi, M., Nemoto, Y., Noguchi, S., et al. (2018). Oncolytic reovirus therapy: Pilot study in dogs with spontaneously occurring tumours. Vet. Comp. Oncol. *16*, 229–238.
20. Clements, D., Helson, E., Gujar, S.A., and Lee, P.W. (2014). Reovirus in cancer therapy: an evidence-based review. Oncolytic Virother. *3*, 69–82.
21. Golding, S.E., Rosenberg, E., Valerie, N., Hussaini, I., Frigerio, M., Cockcroft, X.F., Chong, W.Y., Hummersone, M., Rigoreau, L., Menear, K.A., et al. (2009). Improved ATM kinase inhibitor KU-60019 radiosensitizes glioma cells, compromises insulin, AKT and ERK prosurvival signaling, and inhibits migration and invasion. Mol. Cancer Ther. *8*, 2894–2902.
22. Clarke, P., Richardson-Burns, S.M., DeBiasi, R.L., and Tyler, K.L. (2005). Mechanisms of apoptosis during reovirus infection. Curr. Top. Microbiol. Immunol. *289*, 1–24.
23. Poggioli, G.J., Dermody, T.S., and Tyler, K.L. (2001). Reovirus-induced sigma1s-dependent G(2)/M phase cell cycle arrest is associated with inhibition of p34(cdc2). J. Virol. *75*, 7429–7434.
24. Maitra, R., Seetharam, R., Tesfa, L., Augustine, T.A., Klampfer, L., Coffey, M.C., Mariadason, J.M., and Goel, S. (2014). Oncolytic reovirus preferentially induces apoptosis in KRAS mutant colorectal cancer cells, and synergizes with irinotecan. Oncotarget *5*, 2807–2819.
25. Twigger, K., Vidal, L., White, C.L., De Bono, J.S., Bhide, S., Coffey, M., Thompson, B., Vile, R.G., Heinemann, L., Pandha, H.S., et al. (2008). Enhanced in vitro and in vivo cytotoxicity of combined reovirus and radiotherapy. Clin. Cancer Res. *14*, 912–923.
26. Sei, S., Mussio, J.K., Yang, Q.E., Nagashima, K., Parchment, R.E., Coffey, M.C., Shoemaker, R.H., and Tomaszewski, J.E. (2009). Synergistic antitumor activity of oncolytic reovirus and chemotherapeutic agents in non-small cell lung cancer cells. Mol. Cancer *8*, 47.
27. Rankin, J.T., Jr., Eppes, S.B., Antczak, J.B., and Joklik, W.K. (1989). Studies on the mechanism of the antiviral activity of ribavirin against reovirus. Virology *168*, 147–158.
28. Stiff, A., Caserta, E., Sborov, D.W., Nuovo, G.J., Mo, X., Schlotter, S.Y., Canella, A., Smith, E., Badway, J., Old, M., et al. (2016). Histone Deacetylase Inhibitors Enhance the Therapeutic Potential of Reovirus in Multiple Myeloma. Mol. Cancer Ther. *15*, 830–841.
29. Kelly, K.R., Espitia, C.M., Zhao, W., Wendlandt, E., Tricot, G., Zhan, F., Carew, J.S., and Nawrocki, S.T. (2015). Junctional adhesion molecule-A is overexpressed in advanced multiple myeloma and determines response to oncolytic reovirus. Oncotarget *6*, 41275–41289.
30. Alain, T., Kim, M., Johnston, R.N., Urbanski, S., Kossakowska, A.E., Forsyth, P.A., and Lee, P.W. (2006). The oncolytic effect in vivo of reovirus on tumour cells that have survived reovirus cell killing in vitro. Br. J. Cancer *95*, 1020–1027.

31. Alain, T., Kim, T.S., Lun, X., Liacini, A., Schiff, L.A., Senger, D.L., and Forsyth, P.A. (2007). Proteolytic disassembly is a critical determinant for reovirus oncolysis. Mol. Ther. *15*, 1512–1521.

32. Marcato, P., Shmulevitz, M., Pan, D., Stoltz, D., and Lee, P.W. (2007). Ras transformation mediates reovirus oncolysis by enhancing virus uncoating, particle infectivity, and apoptosis-dependent release. Mol. Ther. *15*, 1522–1530.

33. Hiller, B.E., Berger, A.K., and Danthi, P. (2015). Viral gene expression potentiates reovirus-induced necrosis. Virology *484*, 386–394.

34. Passaro, C., Abagnale, A., Libertini, S., Volpe, M., Botta, G., Cella, L., Pacelli, R., Halldèn, G., Gillespie, D., and Portella, G. (2013). Ionizing radiation enhances dl922-947-mediated cell death of anaplastic thyroid carcinoma cells. Endocr. Relat. Cancer *20*, 633–647.

35. Sinclair, A., Yarranton, S., and Schelcher, C. (2006). DNA-damage response pathways triggered by viral replication. Expert Rev. Mol. Med. *8*, 1–11.

36. Hau, P.M., Deng, W., Jia, L., Yang, J., Tsurumi, T., Chiang, A.K.S., Huen, M.S., and Tsao, S.W. (2015). Role of ATM in the formation of the replication compartment during lytic replication of Epstein-Barr virus in nasopharyngeal epithelial cells. J. Virol. *89*, 652–668.

37. Kozlov, S.V., Graham, M.E., Jakob, B., Tobias, F., Kijas, A.W., Tanuji, M., Chen, P., Robinson, P.J., Taucher-Scholz, G., Suzuki, K., et al. (2011). Autophosphorylation and ATM activation: additional sites add to the complexity. J. Biol. Chem. *286*, 9107–9119.

38. Mainou, B.A., and Dermody, T.S. (2012). Transport to late endosomes is required for efficient reovirus infection. J. Virol. *86*, 8346–8358.

39. Sturzenbecker, L.J., Nibert, M., Furlong, D., and Fields, B.N. (1987). Intracellular digestion of reovirus particles requires a low pH and is an essential step in the viral infectious cycle. J. Virol. *61*, 2351–2361.

40. Blum, J.S., Fiani, M.L., and Stahl, P.D. (1991). Proteolytic cleavage of ricin A chain in endosomal vesicles. Evidence for the action of endosomal proteases at both neutral and acidic pH. J. Biol. Chem. *266*, 22091–22095.

41. Authier, F., Posner, B.I., and Bergeron, J.J. (1996). Endosomal proteolysis of internalized proteins. FEBS Lett. *389*, 55–60.

42. Roulstone, V., Twigger, K., Zaidi, S., Pencavel, T., Kyula, J.N., White, C., McLaughlin, M., Seth, R., Karapanagiotou, E.M., Mansfield, D., et al. (2013). Synergistic cytotoxicity of oncolytic reovirus in combination with cisplatin-paclitaxel doublet chemotherapy. Gene Ther. *20*, 521–528.

43. Heinemann, L., Simpson, G.R., Boxall, A., Kottke, T., Relph, K.L., Vile, R., Melcher, A., Prestwich, R., Harrington, K.J., Morgan, R., and Pandha, H.S. (2011). Synergistic effects of oncolytic reovirus and docetaxel chemotherapy in prostate cancer. BMC Cancer *11*, 221.

44. Hamano, S., Mori, Y., Aoyama, M., Kataoka, H., Tanaka, M., Ebi, M., Kubota, E., Mizoshita, T., Tanida, S., Johnston, R.N., et al. (2015). Oncolytic reovirus combined with trastuzumab enhances antitumor efficacy through TRAIL signaling in human HER2-positive gastric cancer cells. Cancer Lett. *356* (2 Pt B), 846–854.

45. Kelly, K.R., Espitia, C.M., Mahalingam, D., Oyajobi, B.O., Coffey, M., Giles, F.J., Carew, J.S., and Nawrocki, S.T. (2012). Reovirus therapy stimulates endoplasmic reticular stress, NOXA induction, and augments bortezomib-mediated apoptosis in multiple myeloma. Oncogene *31*, 3023–3038.

46. Li, H., Baskaran, R., Krisky, D.M., Bein, K., Grandi, P., Cohen, J.B., and Glorioso, J.C. (2008). Chk2 is required for HSV-1 ICP0-mediated G2/M arrest and enhancement of virus growth. Virology *375*, 13–23.

47. Alekseev, O., Donovan, K., and Azizkhan-Clifford, J. (2014). Inhibition of ataxia telangiectasia mutated (ATM) kinase suppresses herpes simplex virus type 1 (HSV-1) keratitis. Invest. Ophthalmol. Vis. Sci. *55*, 706–715.

48. Machida, K., Cheng, K.T.H., Lai, C.K., Jeng, K.S., Sung, V.M.H., and Lai, M.M.C. (2006). Hepatitis C virus triggers mitochondrial permeability transition with production of reactive oxygen species, leading to DNA damage and STAT3 activation. J. Virol. *80*, 7199–7207.

49. Ryan, E.L., Hollingworth, R., and Grand, R.J. (2016). Activation of the DNA Damage Response by RNA Viruses. Biomolecules *6*, 2.

50. Kim, M., Williamson, C.T., Prudhomme, J., Bebb, D.G., Riabowol, K., Lee, P.W., Lees-Miller, S.P., Mori, Y., Rahman, M.M., McFadden, G., and Johnston, R.N. (2010). The viral tropism of two distinct oncolytic viruses, reovirus and myxoma virus, is modulated by cellular tumor suppressor gene status. Oncogene *29*, 3990–3996.

51. Ebert, D.H., Deussing, J., Peters, C., and Dermody, T.S. (2002). Cathepsin L and cathepsin B mediate reovirus disassembly in murine fibroblast cells. J. Biol. Chem. *277*, 24609–24617.

52. Thirukkumaran, C.M., Shi, Z.Q., Luider, J., Kopciuk, K., Gao, H., Bahlis, N., Neri, P., Pho, M., Stewart, D., Mansoor, A., and Morris, D.G. (2012). Reovirus as a viable therapeutic option for the treatment of multiple myeloma. Clin. Cancer Res. *18*, 4962–4972.

53. Huang, W.-R., Chi, P.-I., Chiu, H.-C., Hsu, J.-L., Nielsen, B.L., Liao, T.-L., and Liu, H.J. (2017). Avian reovirus p17 and σA act cooperatively to downregulate Akt by suppressing mTORC2 and CDK2/cyclin A2 and upregulating proteasome PSMB6. Sci. Rep. *7*, 5226.

54. Kemp, V., Dautzenberg, I.J.C., Limpens, R.W., van den Wollenberg, D.J.M., and Hoeben, R.C. (2017). Oncolytic Reovirus Infection Is Facilitated by the Autophagic Machinery. Viruses *9*, 266.

55. Onishi, K., Shibutani, S., Goto, N., Maeda, Y., and Iwata, H. (2019). Amino acid starvation accelerates replication of Ibaraki virus. Virus Res. *260*, 94–101.

56. Biddlestone-Thorpe, L., Sajjad, M., Rosenberg, E., Beckta, J.M., Valerie, N.C.K., Tokarz, M., Adams, B.R., Wagner, A.F., Khalil, A., Gilfor, D., et al. (2013). ATM kinase inhibition preferentially sensitizes p53-mutant glioma to ionizing radiation. Clin. Cancer Res. *19*, 3189–3200.

57. Pike, K.G., Barlaam, B., Cadogan, E., Campbell, A., Chen, Y., Colclough, N., Davies, N.L., de-Almeida, C., Degorce, S.L., Didelot, M., et al. (2018). The Identification of Potent, Selective, and Orally Available Inhibitors of Ataxia Telangiectasia Mutated (ATM) Kinase: The Discovery of AZD0156 (8-{6-[3-(Dimethylamino)propoxy]pyridin-3-yl}-3-methyl-1-(tetrahydro-2 H-pyran-4-yl)-1,3-dihydro-2 H-imidazo[4,5- c]quinolin-2-one). J. Med. Chem. *61*, 3823–3841.

58. Vecchio, D., Daga, A., Carra, E., Marubbi, D., Raso, A., Mascelli, S., Nozza, P., Garrè, M.L., Pitto, F., Ravetti, J.L., et al. (2015). Pharmacokinetics, pharmacodynamics and efficacy on pediatric tumors of the glioma radiosensitizer KU60019. Int. J. Cancer *136*, 1445–1457.

59. Inoue, K., Ohashi, E., Kadosawa, T., Hong, S.H., Matsunaga, S., Mochizuki, M., Nishimura, R., and Sasaki, N. (2004). Establishment and characterization of four canine melanoma cell lines. J. Vet. Med. Sci. *66*, 1437–1440.

60. Bianco, S.R., Sun, J., Fosmire, S.P., Hance, K., Padilla, M.L., Ritt, M.G., Getzy, D.M., Duke, R.C., Withrow, S.J., Lana, S., et al. (2003). Enhancing antimelanoma immune responses through apoptosis. Cancer Gene Ther. *10*, 726–736.

61. Yoshitake, R., Saeki, K., Watanabe, M., Nakaoka, N., Ong, S.M., Hanafusa, M., Choisunirachon, N., Fujita, N., Nishimura, R., and Nakagawa, T. (2017). Molecular investigation of the direct anti-tumour effects of nonsteroidal anti-inflammatory drugs in a panel of canine cancer cell lines. Vet. J. *221*, 38–47.

62. Sanjana, N.E., Shalem, O., and Zhang, F. (2014). Improved vectors and genome-wide libraries for CRISPR screening. Nat. Methods *11*, 783–784.

OMTO, Volume *15*

Supplemental Information

Combination Therapy with Reovirus and ATM Inhibitor Enhances Cell Death and Virus Replication in Canine Melanoma

Masaya Igase, Shusaku Shibutani, Yosuke Kurogouchi, Noriyuki Fujiki, Chung Chew Hwang, Matt Coffey, Shunsuke Noguchi, Yuki Nemoto, and Takuya Mizuno

Supplemental Information

Figure S1. Drug screening in a reovirus-infected canine melanoma cell line.

To identify drugs that potentiate reovirus cytotoxicity, we screened SCADS inhibitor kits (Kits 1, 2, and 3) comprising a total of 285 compounds. CMeC1 cells were treated with 10 μM of each inhibitor alone (x-axis), or each inhibitor and reovirus (MOI 100) (y-axis) for 48 hr, followed by the addition of the CCK-8 reagent. Both axes indicated the % of cell proliferation as compared with the untreated cells. The diamond-dots, the triangle, and the circle, represented each compound, DMSO, and KU55933-treated samples, respectively. KU55933 alone showed no effect on cell proliferation by itself (x-axis), but combination with reovirus yielded more cytotoxicity (y-axis).

Figure S2. ATM inhibitor KU55933 enhances reovirus-induced cell growth inhibition in the CMeC1 canine melanoma cell line.

To evaluate cell proliferation, a canine melanoma cell line (CMeC1) was treated with reovirus (MOI 100) and KU55933 (indicated concentration) for 48 hr before adding the CCK-8 reagent. Data are expressed as the mean ± SD of three independent experiments. *p* values were calculated for the comparison between reovirus alone and reovirus combined with KU55933. To focus on the additional effects provided by KU55933, significance was tested only where no significant difference was observed between mock control and KU55933 alone. Tukey-Kramer test, $*p < 0.05$.

Figure S3. *ATM* knock-out has various effects on the cell growth in canine melanoma cell lines.

To assess the rate of cell growth, *ATM* knock-out (two clones) and wild type canine melanoma cell lines (CMeC1, KMeC, CMM10, and CMM12) were seeded in triplicates and incubated for 48 hr before adding the CCK-8 reagent to determine the cell proliferation. The Y-axis indicates the cell proliferation relative to that observed at the 0 hr time point. Mean ± SD are shown from three independent experiments. Tukey-Kramer test, $*p < 0.05$, $**p < 0.01$.

Figure S4. The expression levels of reoviral proteins are increased by KU60019 treatment.

Reovirus structural proteins were detected using anti-reovirus polyclonal antibody. Cell lysates were collected from CMeC1 and KMeC cells treated as indicated. Actin was used as a protein loading control.

Figure S5. The expression level of JAM-A does not increase by KU60019 treatment.

CMeC1 were treated with KU60019 (2.5 μM) for 1-hr and 24-hr. To evaluate the surface expression of JAM-A, flow cytometric analysis was performed. Harvested cells were stained with primary antibodies for isotype control (red) and anti-JAM-A antibody (blue), and followed by a secondary antibody for Dylight488-conjugated anti-mouse IgG antibody. Representative data from two independent experiments are shown.

Figure S6. The combination of KU60019 and ISVPs enhances cell growth inhibition in a canine melanoma cell line.

ISVPs were generated using chymotrypsin (see *Methods*). To evaluate cell proliferation, cells of the canine melanoma cell line CMeC1 were treated with ISVPs (MOI 10) and KU60019 (indicated concentration) for 48 hr before adding the CCK-8 reagent. Data are expressed as the mean ± SD from three independent experiments. *p* values were calculated for the comparison between ISVPs alone and ISVPs combined with KU60019. To focus on the additional effects provided by KU60019, significance was tested only where no significant difference was observed between mock control and KU60019 alone. Tukey-Kramer test, $*p < 0.05$, $**p < 0.01$.

Figure S7. Reovirus does not induce the DNA damage response in a canine melanoma cell line.

The levels of phopho-p53 and total p53 were determined by western blotting of lysates from CMeC1 cells treated for the indicated times with reovirus (MOI 100) and KU60019 (2.5 μM). MDCK (Madin-Darby canine kidney epithelial cells) treated with doxorubicin (Dox; MP BIOMEDICALS, LLC, Santa Ana, CA; 0.5 μM) for 12 hr was used as a positive control for DNA damage response. Actin was used as a protein loading control.

Figure S1

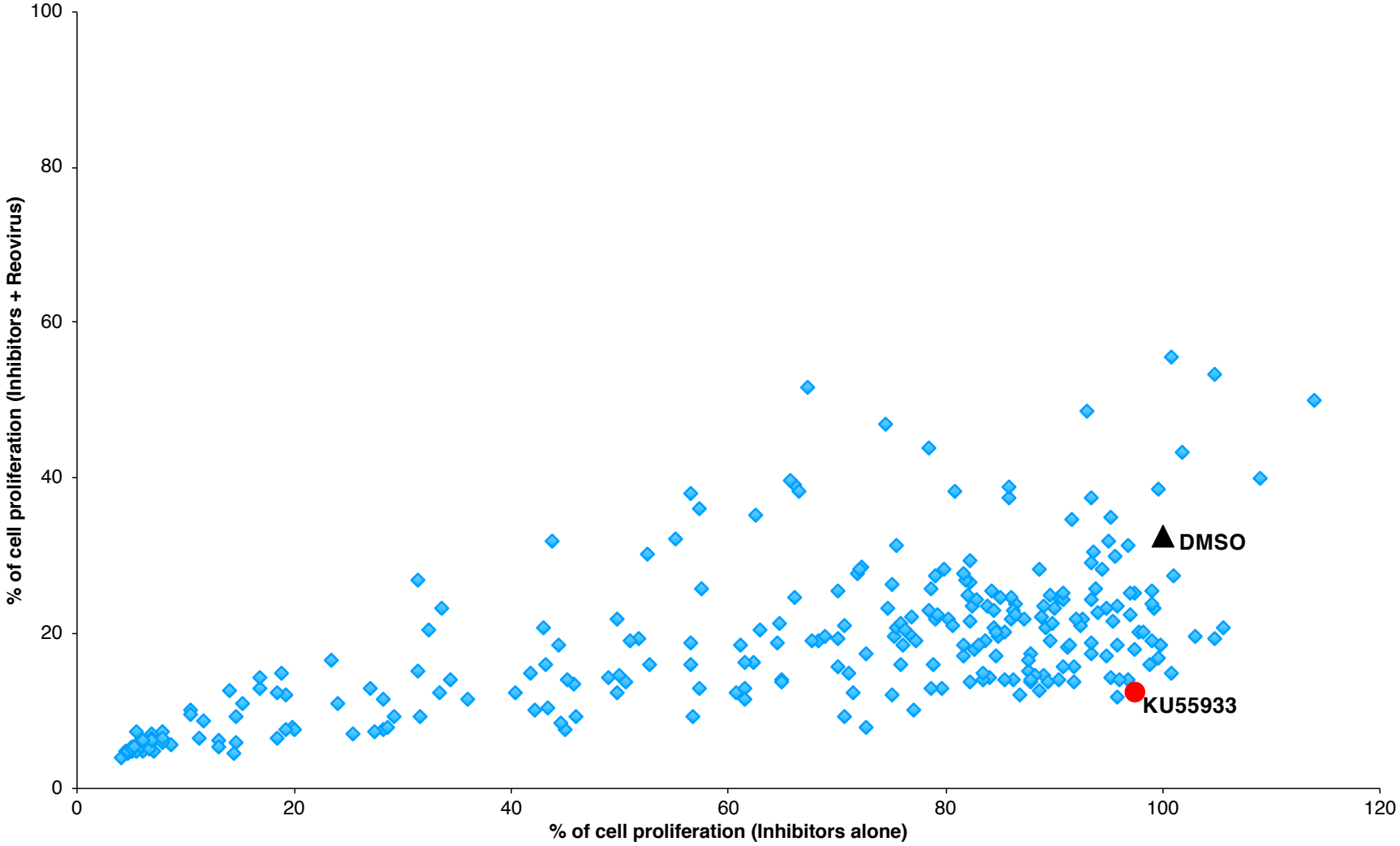
100
80
60
40
20
0
% of cell proliferation (Inhibitors + Reovirus)
0
20
40
60
80
100
120
% of cell proliferation (Inhibitors alone)
DMSO
KU55933

Figure S2

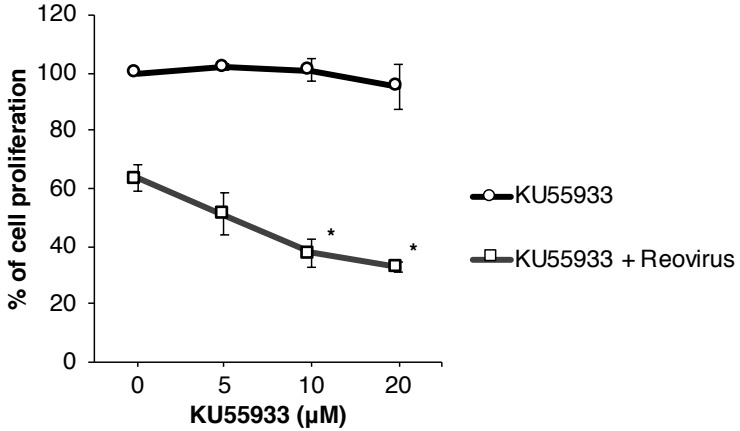
120
100
80
60
40
20
0
% of cell proliferation
0
5
10
20
KU55933 (μM)
*
*
KU55933
KU55933 + Reovirus

Figure S3

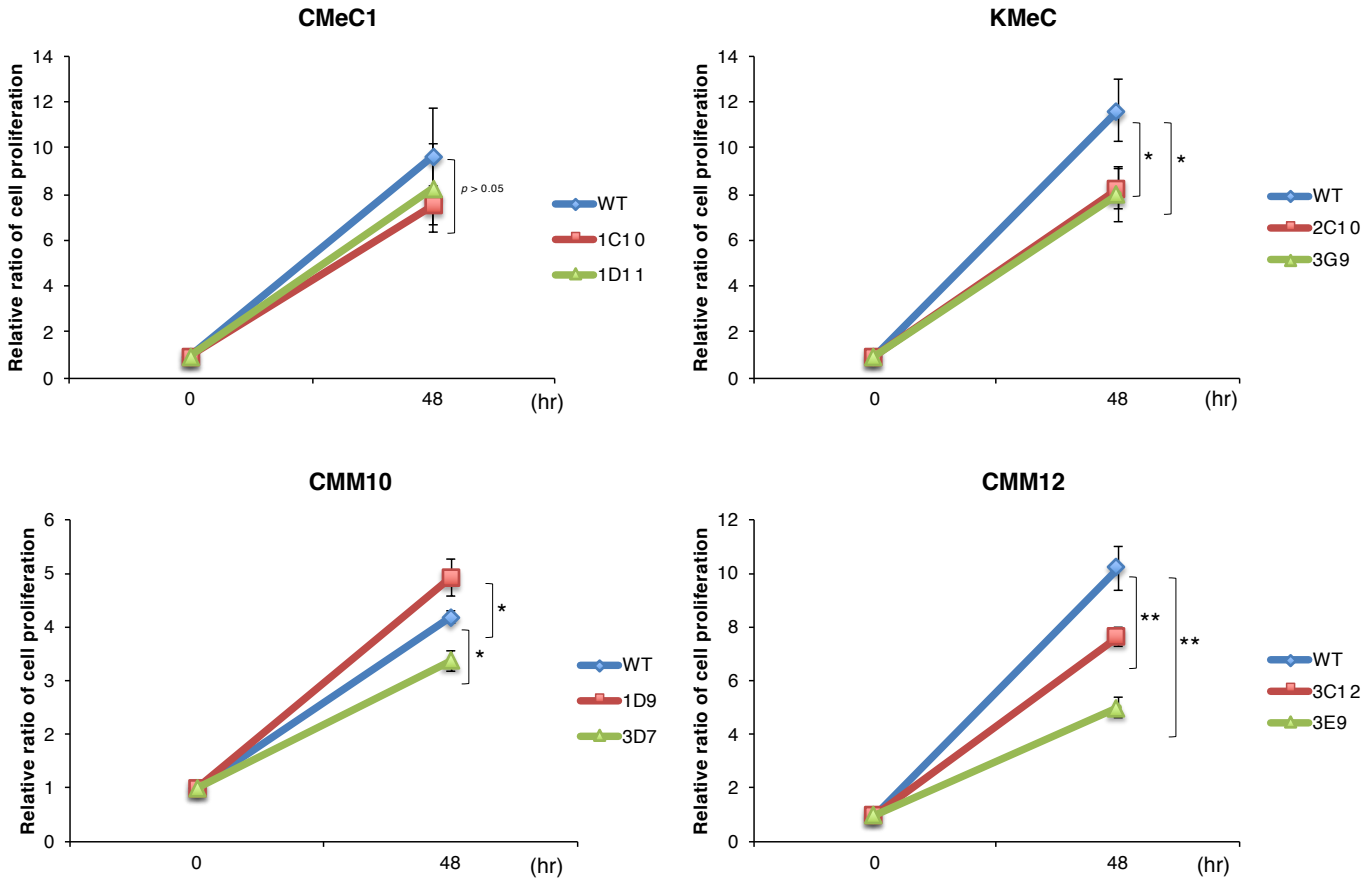
CMeC1
Relative ratio of cell proliferation
p > 0.05
WT
1C10
1D11
0
48
(hr)
KMeC
*
*
WT
2C10
3G9
CMM10
*
*
WT
1D9
3D7
CMM12
**
**
WT
3C12
3E9

Figure S4

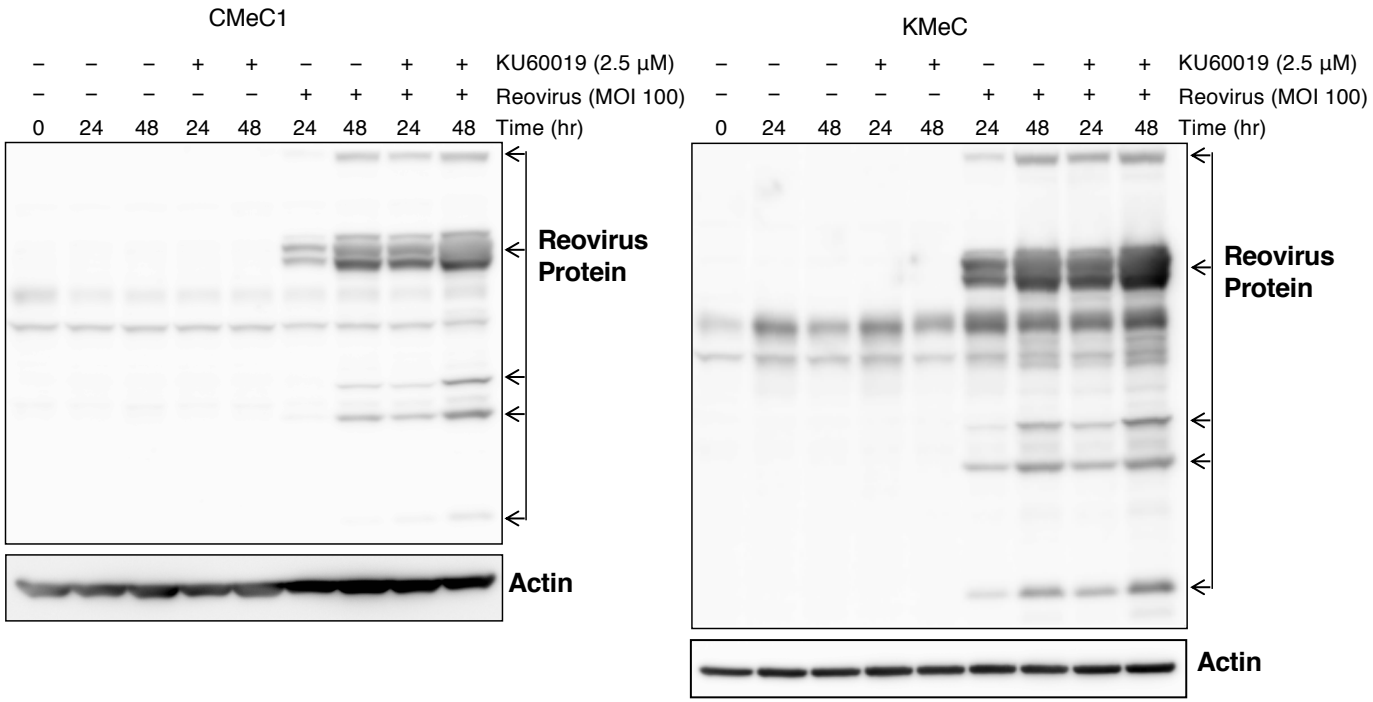
CMeC1
KMeC
– – – + + – – + + KU60019 (2.5 μM)
– – – – – + + + + Reovirus (MOI 100)
0 24 48 24 48 24 48 24 48 Time (hr)
Reovirus Protein
Actin

Figure S5

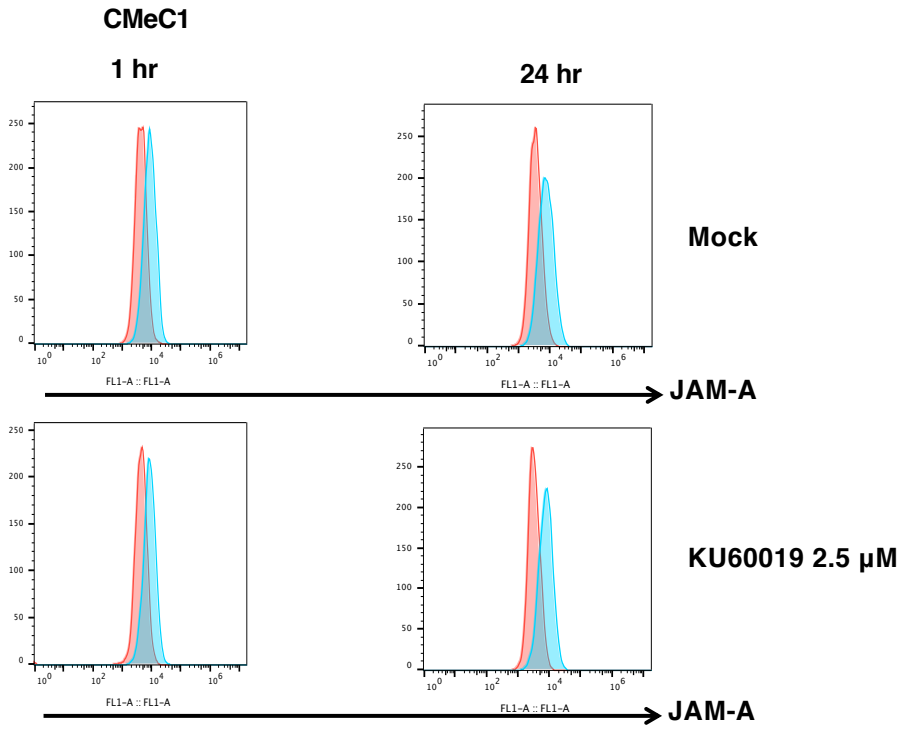

Figure S6

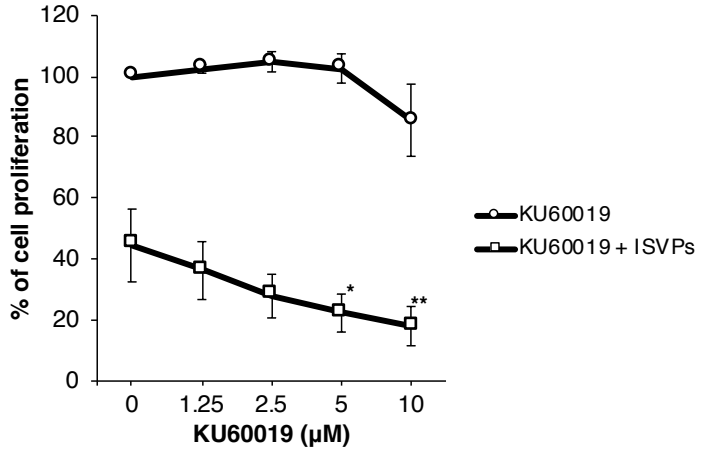
120
100
80
60
40
20
0
% of cell proliferation
0
1.25
2.5
5
10
KU60019 (μM)
*
**
KU60019
KU60019 + ISVPs

Figure S7

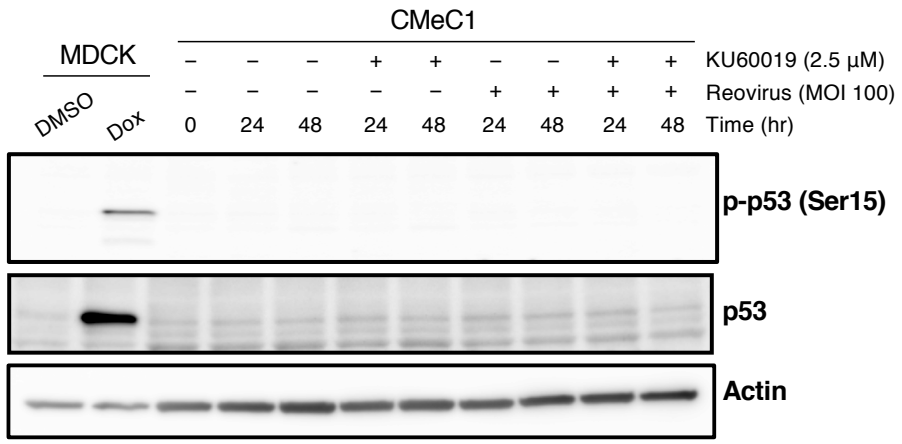
CMeC1
MDCK
KU60019 (2.5 μM)
Reovirus (MOI 100)
DMSO
Dox
Time (hr)
p-p53 (Ser15)
p53
Actin

Table S1. Antibodies are used for the western blotting

No	Antibody	Product no.	Source
1	Rabbit monoclonal anti-cleaved caspase-3(Asp175)	#9661	Cell Signaling Technology, Danvers, MA
2	Rabbit polyclonal anti-cdc2	#77055	Cell Signaling Technology
3	Rabbit polyclonal anti-p21	sc-397	Santa Cruz Biotechnology, Dallas, TX
4	Rabbit polyclonal anti-reovirus	-	Produced by our laboratory
5	Mouse monoclonal anti-ATM	sc-377293	Santa Cruz Biotechnology
6	Mouse monoclonal anti-phospho-ATM(Ser1981)	NB100-306	Novus Biologicals, Littleton, CO
7	Mouse monoclonal anti-p53	ADI-KAM-CC002	Enzo Life Science, Farmingdale, NY
8	Rabbit monoclonal anti-phospho-p53(Ser15)	#9284	Cell Signaling Technology
9	Mouse monoclonal anti-Vinculin	14-9777-80	eBioscience, San Diego, CA
10	Mouse monoclonal anti-beta-actin	A2228	Sigma-Aldrich, St. Louis, MO
11	Mouse monoclonal anti-JAM-A	sc-53623	Santa Cruz Biotechnology
12	Mouse IgG1 kappa, isotype control	#15267367	eBioscience
13	Goat anti-mouse IgG (minimal x-reactivity) -DyLight™ 488	#405310	BioLegend, San Diego, CA
14	Goat anti-mouse IgG-HRP	STAR117P	Bio-rad Laboratories, Hercules, CA
15	Donkey anti-rabbit IgG-HRP	711-035-152	Jackson ImmunoResearch Laboratories, West Grove, PA